Oxidation of Aqueous Sulfide Solutions by Dioxygen Part II: Catalysis by Soluble and Immobilized Cobalt(II) Phthalocyanines

Holger Fischer, Günter Schulz-Ekloff, and Dieter Wöhrle*

The oxidation of sulfide in oxygen-saturated aqueous solutions is accelerated by dissolved or silica-bonded cobalt phthalocyanines. On the basis of thermodynamical considerations it is postulated that the catalyst enhances the formation of disulfide as the initial elementary reaction step. The following reaction steps are largely unaffected by the catalyst, as indicated by a product ratio sulfate/thiosulfate = 0.86, comparable to that of the uncatalyzed autoxidation. A Langmuir-Hinshelwood formalism is developed for the catalytic reaction step and is demonstrated to fit best with the kinetics. In addition, from the kinetic data free enthalpies for the adsorption of HS^- (i) at the dissolved phthalocyanine ($\Delta G = -17.6$ kJ/mole) and (ii) at the immobilized complex ($\Delta G = -20.0$ kJ/mole) are calculated.

1 Introduction

Process gases of the petrochemical industry are often cleaned by alkaline washing, resulting in waste solutions containing sulfide as a pollutant. Cobalt phthalocyanines, which are proven catalysts for the oxidation of mercaptans [1], have been tested for the oxidation of sulfide [2–7]. In principle, phthalocyanines (structure see Fig. 1) are appropriate materials for catalysis under ambient conditions, since they exhibit sufficient thermal stability and resistance towards oxidants, acids, and bases [8, 9]. They can exhibit high activity and stability not only as soluble but also as immobilized catalysts, where the heterogenization can comprise adsorption or impregnation as well as covalent or coordinative bonding at the carrier [7, 10–13].

The role of the phthalocyanine catalyst in the sulfide oxidation sequence, which proceeds also in the autoxidation process without catalyst, is not clear. The preferential formation of thiosulfate is reported [4, 5]. As an initial elementary step the adsorption of HS^- [2, 6] or of O_2 [3] to the cobalt center of the complex is assumed. The kinetics have been modelled by power rate laws [2] or a Michaelis-Menten equation [3]. It is the aim of this contribution to elucidate the role of the catalyst in the oxidation of sulfide studying the kinetics and selectivities under conditions which were also applied for the autoxidation of sulfide without catalysts [14].

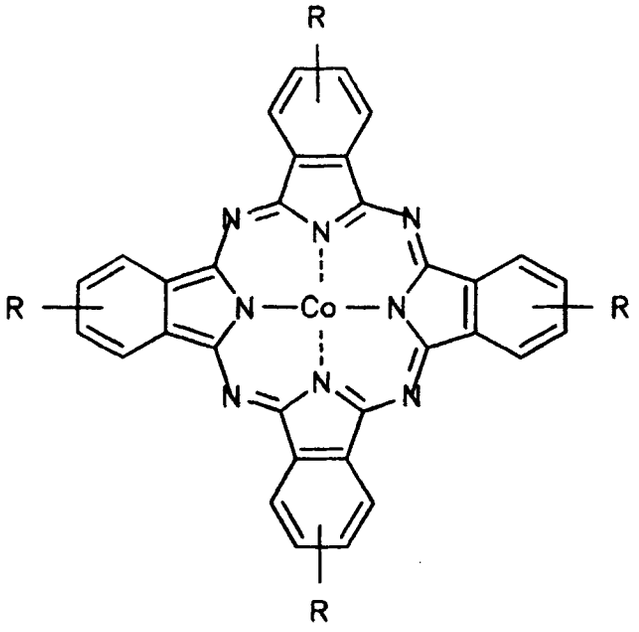

Figure 1. Structure of used cobalt(II) phthalocyanine, R = $-SO_3Na$ or $-NH_2$.

2 Experimental

2.1 Apparatus and Chemicals

All sulfide oxidation experiments were carried out at 298 ± 0.1 K in a thermostated glass reactor, as described in a preceeding article on the uncatalyzed autoxidation of sulfide [14]. The constant total reactor volume of 600 mL contained 120 mL borate buffer for the experiments at pH 9 or aqueous 1 M NaOH for studies at pH 14, 10–50 mL of fresh sulfide stock solution (0.7–0.8 M), added immediately at the start of a kinetic experiment from a storage burette, 0.18–17.6 μM of the soluble

* Dr. Holger Fischer (present address: Faserinstitut Bremen e.V. –FIBRE–, P.O. Box 105807, D-28058 Bremen), Prof. Dr. Günter Schulz-Ekloff (author to whom correspondence should be addressed), Institut für Angewandte und Physikalische Chemie, Universität Bremen, FB II, P.O. Box 330440, D-28334 Bremen, and Prof. Dr. Dieter Wöhrle, Institut für Organische und Makromolekulare Chemie, Universität Bremen, FB II, P.O. Box 330440, D-28334 Bremen, Germany.

0930-7516/97/0912-0624 $17.50+.50/0

phthalocyanine or 0.05–1.7 μM of the immobilized complex suspended in the solution mixture, and deionized water or aqueous 1 M NaOH for the experiments at pH 14, added for the balance of the 600 mL. The kinetics were followed continuously via the oxygen consumption as well as discontinuously via the sulfide conversion measured by a HPLC system (Merck) being connected online to the reactor. All chemicals used were of reagent grade. Stock solutions of sodium sulfide as well as calibration standards for the HPLC from these solutions were prepared as described previously [14]. Sulfide, polysulfides, sulfite, and thiosulfate are detectable by UV [15]. Sulfide and thiosulfate were quantitatively determined by HPLC. Sulfite and polysulfides were below any detection limits. Elemental sulfur is a stable colloid up to ~5 μM [16], and larger concentrations appear as precipitate. Sulfate was identified by a modified gravimetrical method as $BaSO_4$ [14].

2.2 Catalysts

Soluble cobalt(II)-tetrasulfophthalocyanine was prepared from the monosodium salt of 4-sulfophthalic acid [17]. The resulting tetrasodium salt of 2,9,16,23-cobalt(II)-phthalocyanine-tetrasulfonic acid ($CoPc(SO_3Na)_4$) was used as catalyst.

Cobalt(II)-tetraaminophthalocyanine, coordinately immobilized on surface-modified silica (SilIm-$CoPc(NH_2)_4$), was prepared by the method of Buck et al. [12, 18]. The first step is the modification of silica (Merck Fractosil 2500™: grain size ≈80 μm, pore diameter >250 nm, surface area (BET)=8.3 $m^2 g^{-1}$) with 3-(chloropropyl)-trimethoxysilane and imidazole:

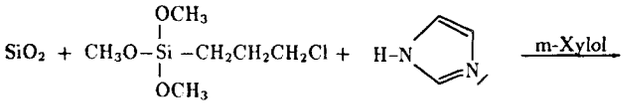

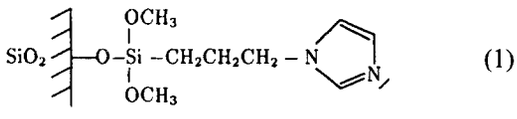

'SilIm'

The second step is the synthesis of cobalt(II)-tetraaminophthalocyanine ($CoPc(NH_2)_4$) by the reaction of $CoCl_2$ with 4-aminophthalodinitrile [18], followed by reduction with Na_2S to the corresponding amine [19]. Final step is the immobilization, performed by adding the modified silica to a suspension of $CoPc(NH_2)_4$ in DMF and stirring 4 h at 353 K [12] (s. scheme SilIm-$CoPc(NH_2)_4$).

The stoichiometry of the chelates was checked by elemental analysis (C,N,H). The chelate content of the SilIm-$CoPc(NH_2)_4$ sample is 2.6 μmoles g^{-1}, measured by cobalt-AAS (atomic absorption spectroscopy).

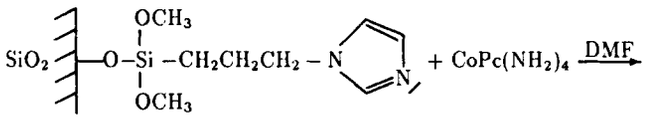

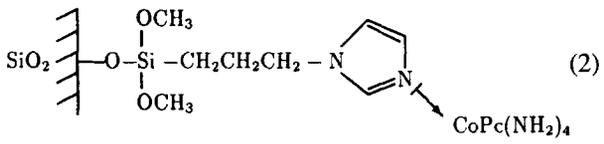

'SilIm-$CoPc(NH_2)_4$'

2.3 Kinetics

All initial kinetics with a reaction order ≠0 were treated as pseudo-first-order reactions. The initial rates of O_2 conversion were calculated by the method presented in part I [14]. The non-catalytic autoxidation rate ($v_{0,\text{ non-cat.}}$), evaluated separately and yielding $v_{0,Na_2S}=3.04\cdot10^{-5}(c_{0,Na_2S})^{0.79}$ and $v_{0,O_2}=4.03\cdot10^{-5}(c_{0,Na_2S})^{0.72}$, was subtracted from the catalyzed overall conversion. The result is defined as '*effective initial rate*'

$$v_{0,\text{eff.}} \equiv v_0 - v_{0,\text{non-cat.}} \tag{3}$$

Reaction orders in time (n_t) were calculated as already described in [14].

3 Results

3.1 Soluble Catalyst

3.1.1 Sulfide Oxidation at pH 9

The influence of varied initial sulfide concentration (1.3–83 mM) on the conversion kinetics was studied with a constant concentration (1 μmole ≡1.7 μM) of the water-soluble $CoPc(SO_3Na)_4$. The results are summarized in Tab. 1 and are reliable with $r \geq 0.99$.

Table 1. Initial rates v_0 and effective rates $v_{0,\text{eff.}}$ for sulfide oxidation on catalyst $CoPc(SO_3Na)_4$ (1.7 μM) and different initial sulfide concentrations c_0 derived from sulfide **A** and oxygen **B** consumption.

Exp. no.	c_0 [mM]	**A** [μM s^{-1}]		**B** [μM s^{-1}]	
		v_0	$v_{0,\text{eff.}}$	v_0	$v_{0,\text{eff.}}$
1	1.3	0.5	0.3		
2	6.2	3.0	2.5	2.7	1.7
3	13.6	4.1	3.1	8.1	6.3
4[a]	13.7	4.8	3.4	5.2	3.1
5[b]	14.3	5.5	4.3	7.6	5.6
6	19.9	5.6	4.1		
7	27.1	5.7	4.0	8.6	5.7
8	33.4	5.5	3.4	9.8	6.3
9	33.7	5.2	3.1	6.9	3.4
10	42.9	9.9	7.4	12.1	8.0
11	82.9	8.1	3.9	10.6	4.0

a) 1.9 μMol L^{-1} $CoPc(SO_3Na)_4$.
b) 1.8 μMol L^{-1} $CoPc(SO_3Na)_4$.

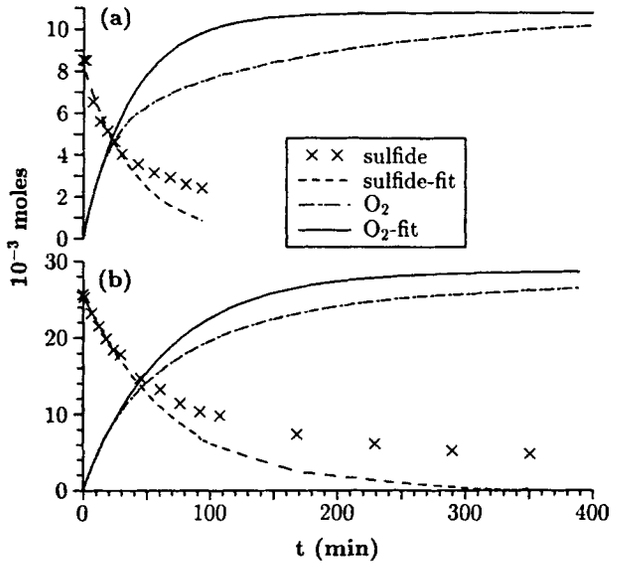

Figure 2. Temporal increase of oxygen consumption and decrease of sulfide concentration on catalyst $CoPc(SO_3Na)_4$ for initial sulfide concentrations of 14.3 mM (**a**) or 42.9 mM (**b**). The fit-functions used for evaluation of the initial reaction rates are included.

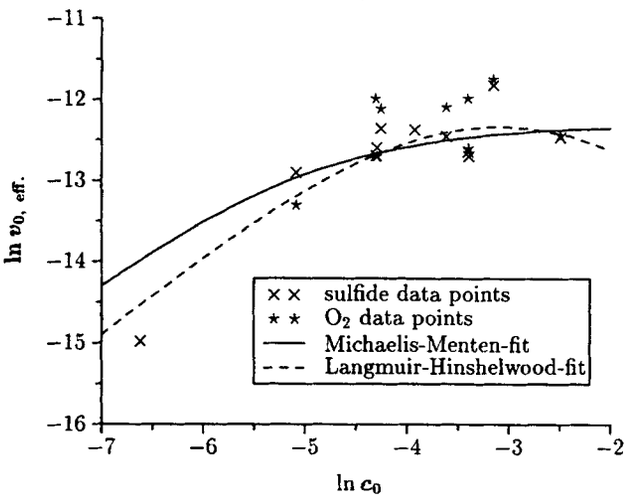

Figure 3. Plot of ln $v_{0,eff.}$ versus ln c_0 on catalyst $CoPc(SO_3Na)_4$ derived from sulfide and oxygen consumption (Tab. 1). The fit-functions obtained by Michaelis-Menten (Eq. (4)) and Langmuir-Hinshelwood formalism (Eq. (9)) are included.

Kinetics are presented exemplarily (Fig. 2) for two experiments (5 and 10, Tab. 1). From a comparison of the overall rates v_0 with the effective catalytic rates $v_{0,eff.}$ or with the differences (cf. Eq. (3)), respectively, representing the uncatalyzed autoxidation rates (Tab. 1), it follows that the catalyst increases the sulfide conversion by a factor of ca. 3 for low c_{0,Na_2S} and ca. 2 for high c_{0,Na_2S} values. The use of a catalyst results in an immediate start of the sulfide oxidation (Fig. 2) without any autocatalytic induction period as observed always for the uncatalyzed reaction [14].

A plot of ln $v_{0,eff.}$ versus ln c_0 (Fig. 3) using the data of Tab. 1 indicates a saturation behavior for higher initial sulfide concentrations, i.e., a reaction order ranging from 1 to 0, which was never observed for the autoxidation reaction. At higher degrees of conversion, however, the reaction patterns approach those of the uncatalyzed reaction. For experiment no. 5 (Tab. 1) with $c_0 = 14.3$ mM a linear least square analysis of ln v_t versus c_t gives $n_t = 2.48 \pm 0.14$, ln $k = -1.27 \pm 0.21$ and $r = 0.984$, i.e., values comparable to the pure autoxidation [14].

The final product distribution is identical to that of the uncatalyzed reaction, i.e., 30% of the sulfide is converted to sulfate and 70% to thiosulfate, resulting in a molar ratio sulfate/thiosulfate = 0.86 with standard deviations of ±10%.

Experiments with varied catalyst concentrations are summarized in Tab. 2. Fig. 4 shows exemplarily the oxygen and sulfide consumption plots for the experiments no. 13 and 15 from Tab. 2 with 0.53 and 17.6 µM catalyst. One can observe the transition from a behavior like the non-catalytic sulfide oxidation with a short induction phase for experiment no. 13 to a reaction order of zero for experiment no. 15 with high catalyst concentration. This means that ex-

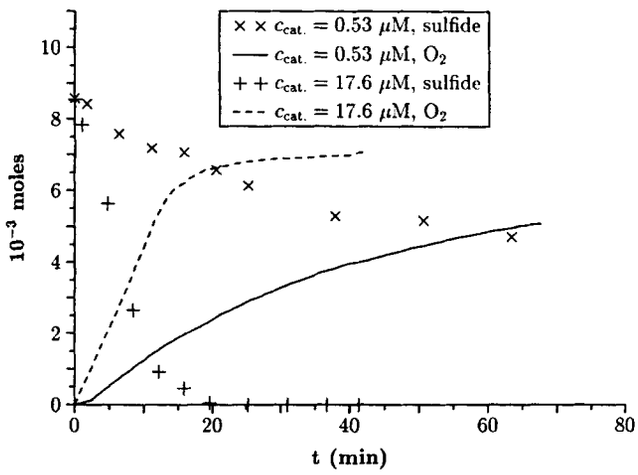

Figure 4. Temporal increase of oxygen consumption and decrease of sulfide concentration on catalyst $CoPc(SO_3Na)_4$ for $c_{cat.} = 17.6$ and 0.53 µM.

Table 2. Initial rates v_0 and effective rates $v_{0,eff.}$ for sulfide oxidation on catalyst $CoPc(SO_3Na)_4$ at constant $c_{0,Na_2S} = 14.3$ mM and different catalyst concentrations $c_{cat.}$ derived from sulfide **A** and oxygen **B** consumption.

Exp. no.	$c_{cat.}$ [µM]	**A** [µM s^{-1}]		**B** [µM s^{-1}]	
		v_0	$v_{0,eff.}$	v_0	$v_{0,eff.}$
12	0.18	1.9	0.9	3.0	1.1
13	0.53	2.6	1.6	4.1	2.2
5[a)]	1.8	5.5	4.5	7.6	5.8
14	5.3	12.4	11.4	12.6	10.8
15	17.6	19.0	18.0	13.0	11.2

a) Result taken from Tab. 1.

periments with $c_{cat} \geq 2$ µM (nos. 14 and 15, Tab. 2) can be considered as zero-order in kinetic calculations. Further, with increasing catalyst concentration (Tab. 2, exp. no. 15) the sulfide conversion rates (Tab. 2, A) are higher than the oxygen consumption rates (Tab. 2, B). Additionally, only in this single experiment sulfur precipitation was observed and the selectivity was strongly changed, i.e., 72% of the sulfide was converted to thiosulfate and only 6% to sulfate. This means that the sulfur production (ca. 22%) reduces the formation of sulfate but not that of thiosulfate.

From a linear least squares fit of ln $v_{0,eff.}$ versus ln $c_{cat.}$ (values from Tab. 2) kinetic coefficients are extracted: $n_{cat}=0.68\pm0.03$, $\ln k=-3.16\pm0.07$, $r=0.998$ for the O_2 consumption, and $n_{cat}=0.77\pm0.05$, $\ln k=-2.14\pm0.12$, $r=0.994$ for sulfide conversion. Only experiment no. 15 exhibited a deviation due to its different kinetics (cf. above) and had to be excluded from this calculation.

3.1.2 Sulfide Oxidation at pH 14

Five experiments have been carried out in unbuffered 1 M NaOH solution with 1.7 µM $CoPc(SO_3Na)_4$ as catalyst. The initial sulfide concentration was varied from 1.5 to 97.5 µM (Tab. 3). The sample circuit was dismounted to prevent any damage to the HPLC system by the strongly basic solution. Thus, only oxygen consumption data could be retrieved from this set of experiments. The resulting plots of total O_2 consumption versus time are shown in Fig. 5. The reaction order in time is obviously zero, and v_0 values were directly calculated by a linear least squares fit. They are listed in Tab. 3, together with corresponding $v_{0,eff.}$ values, calculated from the database of the pure autoxidation [14].

Table 3. Initial rates v_0 and effective rates $v_{0,eff.}$ for sulfide oxidation on catalyst $CoPc(SO_3Na)_4$ (1.7 µM) at pH 14 and different initial sulfide concentrations c_0 derived from oxygen consumption.

Exp. no.	c_0 [mM]	v_0 [µM s^{-1}]	$v_{0,eff.}$ [µM s^{-1}]
16	1.5	4.5	4.3
17	4.4	8.4	7.9
18	15.1	9.5	8.1
19	44.2	10.8	7.3
20	97.5	8.1	1.3

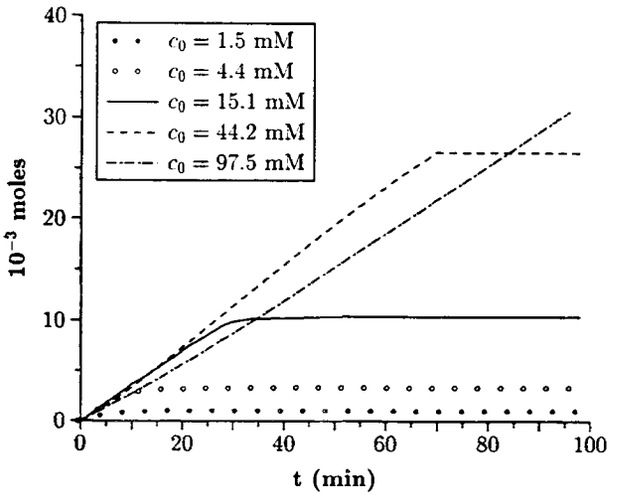

Figure 5. Temporal increase of the O_2 consumption on catalyst $CoPc(SO_3Na)_4$ at pH 14 and initial sulfide concentrations of $c_0=1.4$–97.5 mM.

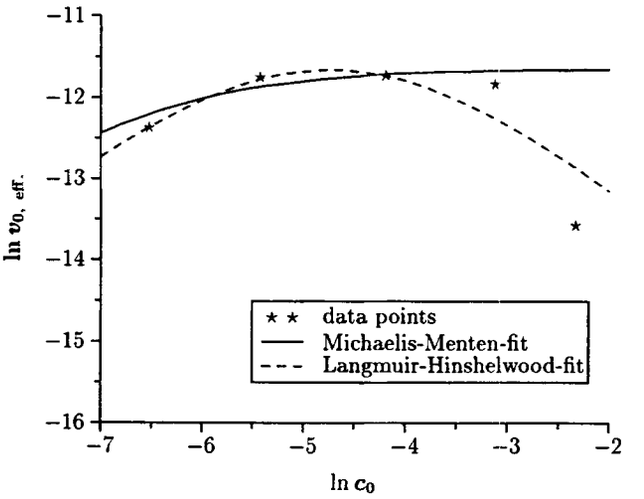

Figure 6. Plot of ln $v_{0,eff.}$ versus ln c_0 from Tab. 3 for experiments at pH 14. The fit-functions obtained by Michaelis-Menten (Eq. (4)) and Langmuir-Hinshelwood formalism (Eq. (9)) are included.

A remarkable result is that the oxygen consumption rate increases at low c_0, then stays nearly constant, and finally strongly decreases at high c_0 values. This effect is strongly enlarged by calculating $v_{0,eff.}$, i.e., the catalytic activity drops nearly down to zero (Tab. 3, no. 20). A double logarithmic plot ln $v_{0,eff.}$ versus ln c_0 (Fig. 6) shows also a saturation effect as observed for the catalyzed reaction at pH 9 (cf. Fig. 3). A diffusion limit for oxygen can be excluded, because higher consumption rates were reached at lower initial concentrations, and the graph for experiment no. 20 (Tab. 3) with $c_{0,Na_2S}=97$ mM shows a lower initial rate than the experiments with lower c_0, but the rate increases during the reaction run.

3.2 Immobilized Catalyst

380 mg of the immobilized catalyst (SilIm-$CoPc(NH_2)_4$, containing 1 µmole phthalocyanine ($\equiv 1.7$ µM) were suspended in the sulfide oxidation solutions; the results are summarized in Tab. 4. A blank experiment using 380 mg support without catalyst exhibited an induction period and resulted in v_0 values comparable to those for the uncatalyzed autoxidation of sulfide [14].

Kinetics of the catalyzed reaction are presented exemplarily for two experiments (22 and 26, Tab. 4) in Fig. 7. Due to linear progress of the initial conversions the evaluation was based on zero-order kinetics. Double logarithmic plots of ln $v_{0,eff.}$ versus ln c_{0,Na_2S} resulted in graphs of a slope

Table 4. Initial rates v_0 and effective rates $v_{0,\text{eff.}}$ for sulfide oxidation on catalyst SilIm-CoPc(NH_2)$_4$ (1.7 μM) and different initial sulfide concentrations c_0 derived from sulfide **A** and oxygen **B** consumption.

Exp. no.	c_0 [mM]	**A** [μM s^{-1}]		**B** [μM s^{-1}]	
		v_0	$v_{0,\text{eff.}}$	v_0	$v_{0,\text{eff.}}$
21	1.6	1.9	1.8		
22	13.3	4.3	3.3	4.5	2.7
23	13.9			4.2	2.4
24	15.8	2.8	1.7	3.0	1.0
25	33.3	3.5	1.5	5.0	1.6
26	54.3	5.3	2.3	6.1	1.2
27[a)]	12.9	1.1	0.13	1.3	–0.4

a) Blank experiment on 380 mg support.

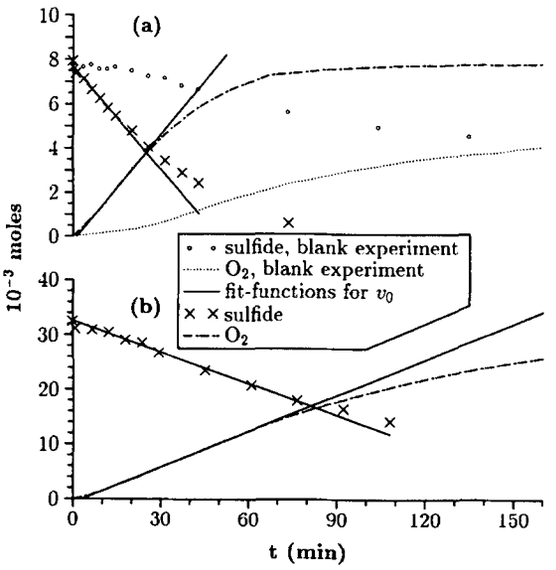

Figure 7. Temporal increase of the oxygen consumption and decrease of the sulfide concentration on catalyst SilIm-CoPc(NH_2)$_4$ for initial sulfide concentrations of 13.3 mM (**a**) or 54.3 mM (**b**). The slope graphs representing the initial reaction rates are included. A blank experiment on surface-modified silica is inserted in (**a**).

Table 5. Initial rates v_0 and effective rates $v_{0,\text{eff.}}$ for sulfide oxidation on catalyst SilIm-CoPc(NH_2)$_4$ at different catalyst concentrations ($c_{\text{cat.}}$) derived from sulfide **A** and oxygen **B** consumption.

Exp. no.	$c_{\text{cat.}}$ [μM]	c_{0,Na_2S} [mM]	**A** [μM s^{-1}]		**B** [μM s^{-1}]	
			v_0	$v_{0,\text{eff.}}$	v_0	$v_{0,\text{eff.}}$
22	1.7	13.3	4.3	3.2	4.5	2.7
28	0.44	12.9	2.2	1.3	3.3	1.6
29	0.22	12.8	1.9	0.9	2.5	0.8
30	0.05	13.1	1.3	0.3	2.1	0.4

close to zero ($n_c = 0.02 \pm 0.14$) indicating a saturation effect of the catalyst in all experiments and over the total range of c_{0,Na_2S} values. A linear least squares fit of the double logarithmic plot of v_t versus c_t, taken from the sulfide consumption graph in Fig. 7(a), resulted in the coefficients $n_t = 0.57 \pm 0.06$ and $\ln k = -10.04 \pm 0.15$ ($r = 0.939$). The molar ratio sulfate/thiosulfate is 0.54. The study of the reaction order in catalyst concentration was only possible with catalyst amounts smaller than the standard value 1.7 μM (Tab. 5). As for the soluble catalyst, reaction orders in catalyst concentration < 1 were found in a double logarithmic plot $\ln v_{0,\text{eff.}}$ versus $\ln c_{\text{cat.}}$: $n_{\text{cat.}} = 0.62 \pm 0.02$, $\ln k = -4.40 \pm 0.07$ and $r = 0.998$.

4 Discussion

4.1 Kinetics

4.1.1 Power Rate Law Modeling

The most striking effect of the catalyst is the elimination of the induction period which always appears in the uncatalyzed autoxidation of sulfide. Obviously, the catalyst can accelerate the formation of disulfide, which has been considered to be the slowest step in the autoxidation reaction for thermodynamical reasons [14].

The catalyzed oxidation exhibits initial reaction orders or reaction orders in concentration (n_c), respectively, close to unity and reaction orders in time (n_t) of ca. 2.5 for moderate initial sulfide concentrations. This behavior resembles that of the pure autoxidation and justifies the power-rate law modeling for the reaction start. The saturation effects appearing at moderate catalyst concentrations and high initial sulfide concentrations (Figs. 3, 6) or at high catalyst concentrations and moderate initial sulfide concentrations (Fig. 4) cannot be modeled by a power-rate law and will be treated in the following section.

4.1.2 Michaelis-Menten Formalism

The kinetics of the catalysis by phthalocyanines have been treated by a Michaelis-Menten equation in the case of thiol [20, 21] as well as sulfide oxidation [6] and can be represented as

$$v_{0,\text{eff.}} = \frac{V\, c_{0,Na_2S}}{K_M + c_{0,Na_2S}} \tag{4}$$

V is the product of the catalyst concentration c_{cat} and the rate constant k, $K_M = (k_2 + k_3)/k_1$ contains the rate constants for the formation of the adsorption complex, ie., forth (k_1) and back (k_2), and of the product (k_3). A Hanes plot of a Michaelis-Menten equation, which is known to be more insensitive to deviations of single data points [22, 23], gives

$$\frac{c_{0,Na_2S}}{v_{0,\text{eff.}}} = \frac{K_M}{V} + \frac{c_{0,Na_2S}}{V} \tag{5}$$

A plot of $c_{0,Na_2S}/v_{0,\text{eff.}}$ versus c_{0,Na_2S} is used for the evaluation of the Michaelis-Menten coefficients K_M, V, and k_3 by a linear least squares fit. The results are listed in

Table 6. Constant K_M, maximum rate V, rate constant of product formation k_3, and reliability r derived from the Michaelis-Menten formalism.

Catalyst	K_M [s^{-1}]	V [$\mu M\ s^{-1}$]	k_3 [s^{-1}]	r
$CoPc(SO_3Na)_4$	0.00587	4.56	2.68	0.923
$SiIIm\text{-}CoPc(NH_2)_4$	0.00175	2.11	1.26	0.931
$CoPc(SO_3Na)_4$ [a]	0.0011	8.77	5.03	0.994 [b]

a) Catalysis at pH 14, data from O_2 consumption.
b) Calculated from the first 4 data points.

Tab. 6. The fits are not satisfying, especially for the results at pH 14 (Fig. 6).

A better fit is achieved by a modified Michaelis-Menten formalism, where the *active* chelate-substrate complex [Pc–HS^-] adds a second substrate molecule to become an *inactive* complex [Pc–$(HS^-)_2$] [23].

$$\frac{1}{v_{0,\mathrm{eff.}}} = \frac{1}{V}\left(1 + \frac{c_{0,Na_2S}}{K_{SS}}\right) + \frac{K_M}{V\, c_{0,Na_2S}} \quad \text{with}$$

$$K_{SS} = \frac{[\mathrm{Pc} - HS^-]\, c_{0,Na_2S}}{[\mathrm{Pc} - (HS^-)_2]} \tag{6}$$

An iterative fitting, i.e., estimation of the coefficient K_{SS}, results in a better matching of the experimental data, but was only performed by trial and error.

The simple Michaelis-Menten formalism represented by Eqs. (4) and (5) is not able to consider reaction orders for the catalyst concentration $\neq 1$, which are found. Moreover, the evaluation of the adsorption coefficient K_{SS}, which is needed for a better fit, requires a high number of very precise measurements over a broad range of concentrations.

4.1.3 Langmuir-Hinshelwood Formalism

In the following a kinetic formalism is developed based on the standard Langmuir-Hinshelwood statement where the reaction rate is proportional to the surface coverage ϑ of the educts on the catalyst surface [24]

$$v = k\, \vartheta_A\, \vartheta_B \cdots \vartheta_i \quad \text{with} \quad \vartheta_A = \frac{K_A p_A}{1 + \sum K_i p_i} \tag{7}$$

It is assumed that the adsorption equilibrium follows Langmuir's isotherm. The most important feature of this approach is, that it allows more than one adsorbate molecule, i.e., HS^- or O_2, to be adsorbed at a phthalocyanine entity. The reaction rate is expressed as change of the mole fraction of sulfide per time

$$-\frac{d\chi_{HS^-}}{dt} = \frac{v_{0,\mathrm{eff.}}}{[H_2O]} \equiv v_0^* \tag{8}$$

The developed rate law has to consider all substances interacting with the phthalocyanine. This is HS^-, O_2 and, in principle, also H_2O and OH^-. The concentration of OH^- is held constant by the buffer, and the changes in H_2O concentration during an experiment are so small that they can be neglected. The resulting rate law is then

$$v_0^* = k\, \frac{K_{HS^-} K_{O_2} \chi_{HS^-} \chi_{O_2}}{(1 + K_{HS^-} \chi_{HS^-} + K_{O_2} \chi_{O_2})^2} \tag{9}$$

A linearized form of Eq. (9) gives

$$\sqrt{\frac{\chi_{HS^-}}{v_0^*}} = \underbrace{\frac{1 + K_{O_2} \chi_{O_2}}{\sqrt{k\, K_{O_2} \chi_{O_2} K_{HS^-}}}}_{\equiv a} + \chi_{HS^-} \underbrace{\sqrt{\frac{K_{HS^-}}{k\, K_{O_2} \chi_{O_2}}}}_{\equiv b} \tag{10}$$

If χ_{HS^-} is varied in a set of experiments, the parameters a and b can be calculated by a linear least squares fit of a plot $\sqrt{\frac{\chi_{HS^-}}{v_0^*}}$ versus χ_{HS^-}, Now can k and K_{HS^-} easily be calculated from a and b

$$K_{HS^-} = \frac{b}{a}\,(1 + K_{O_2} \chi_{O_2}) \tag{11}$$

$$k = \frac{K_{HS^-}}{b^2\, K_{O_2} \chi_{O_2}} \tag{12}$$

The following considerations demonstrate that the second term in Eq. (11) can be neglected. Firstly, χ_{O_2} can be estimated using Henry's law

$$p_A = \chi_A\, \mathrm{Const}_A \tag{13}$$

From the value of Henry's constant for O_2 in water, i.e., $\mathrm{Const}_A = 4.40 \cdot 10^7$ mbar [24], and the experimental partial oxygen pressure $p_{O_2} = 1000$ mbar follows $\chi_{O_2} = 2.27 \cdot 10^{-5}$. This is 1.26 mM, i.e., ca. 100 times more than the maximum O_2 consumption per second measured here. So c_{O_2} can be considered as constant 1.26 mM (cf. [14]).

Secondly, the low χ_{O_2} value could only be counterbalanced by a $K_{O_2} > 10^3$, i.e., ΔG values of the oxygen chemisorption at phthalocyanines >20 kJ mol^{-1}, or even larger values for the enthalpy of adsorption since the entropy change for the adsorption process is positive. Thermal desorption experiments report activation energies for the desorption of chemisorbed oxygen from CuPc and FePc $E_A = 31$–41 kJ mol^{-1} [25], from CoPc $E_A = 2$–15 kJ mol^{-1} [26], and ESR studies reported a binding energy of <2 kJ mol^{-1} [27] for O_2 at CoPc. Assuming that the oxygen desorption reaction is accompanied by an adsorption reaction, a resulting ΔG must be smaller than the E_A values. Thus, $\Delta G \approx -3$ kJ mol^{-1} will be used as representative average value in all further calculations. This gives $K_{O_2} = 3.36$ via $\Delta G = -RT \ln K$. The value of $K_{O_2}\, \chi_{O_2}$ is then only $7.6 \cdot 10^{-5}$, confirming the neglection in Eq. (11).

ΔG values derived by Eq. (11) and the relation $\Delta G = -RT \ln K$, as well as rate constants which are subsequently derived by Eq. (12) are summarized in Tab. 7. The stronger adsorption for HS^- at $SiIIm\text{-}CoPc(NH_2)_4$ as compared to

Table 7. Rate constant k, adsorption constant K_{HS^-}, free enthalpy of adsorption ΔG, and reliability r derived from the Langmuir-Hinshelwood formalism.

Catalyst	k [s^{-1}]	K_{HS^-}	ΔG [kJ $mole^{-1}$]	r
$CoPc(SO_3Na)_4$	0.0042	1214	−17.6	0.915
SilIm-$CoPc(NH_2)_4$	0.0024	3177	−20.0	0.919
$CoPc(SO_3Na)_4$ [a]	0.0082	6360	−21.7	0.999 [b]

a) Experiments at pH 14.
b) Calculated from the first 3 data points.

$CoPc(SO_3Na)_4$ at pH 9 is in agreement with the zero-order kinetics (Fig. 7), pointing to a more strongly covered catalyst.

At pH 14 the enlarged reaction rate at low educt concentrations as well as strong inhibition of the rate of oxidation at high educt concentrations might be caused by participation of more strongly adsorbed S^{2-} ions instead of HS^- ions. As previously discussed in part I [14], S^{2-} ions should be present at this pH in remarkable concentrations.

It can be summarized that the application of a simple Langmuir-Hinshelwood formalism for the modeling of the kinetics of the catalyzed sulfide oxidation gives a better fit of the experimental data and readily explains values for the reaction order $n \neq 1$. The reaction order $\neq 1$ in catalyst concentration can here be explained as a change of the ratio $\chi_{cat.} : \chi_{HS^-}$, influencing the kinetics. In addition, it enables an easy access to thermodynamical data of the educt adsorption equilibria.

The underlying assumption that more than one adsorption site exists at a phthalocyanine unit, which can be considered as a heterogeneous catalyst rather than a homogeneous one, is repeatedly put forward by other scientists [18, 26, 28]. Especially, in the case of the immobilized phthalocyanine systems, e.g., SilIm-$CoPc(NH_2)_4$, where only one axial site of the Co center is accessible for the reaction partners HS^- and O_2, their simultaneous adsorption requires additional sites, presumably located at the nitrogen atoms of the chelate complex.

4.2 Catalyzed Elementary Steps

The most thorough mechanistic considerations on the sulfide oxidation catalyzed by Co(II)Pc have been published by Kotronarou and Hoffmann [6]. The authors postulate an electron transfer from an adsorption complex $[(HS^-)Co(II)Pc]$ to an additionally adsorbed O_2, i.e., $[(HS^-)Co(III)Pc\ (O_2^{\bullet -})]$. The assumed valency change of Co(II)Pc to Co(III)Pc is, however, improbable since the corresponding redox potential is $E_0 = 0.65$ V [29], and cannot reduce the dioxygen to the most probable intermediate H_2O_2, with $E_0 = 0.07$ V ($O_2 + H_2O/OH^- + HO_2^-$) at pH 9 [14].

A weak driving force for the reduction of dioxygen exists, if Co(I)Pc is assumed as intermediate, since $E_0 = 0.05$ V for Co(II)Pc/Co(I)Pc is reported [29]. Co(I)Pc has been found after H_2S adsorption by UV/vis spectroscopy [30] and EPR measurements [31]. A reduction of Co(II)Pc to Co(I)Pc cannot be achieved by direct oxidation of one or two HS^- ions. Both possible reactions do not provide the required low E_0 value [32]

$$HS^{\bullet} + e^- \rightleftharpoons HS^- \qquad E_0 = 1.15\ V \tag{14}$$

$$H_2S_2^{-\bullet} + e^- \rightleftharpoons 2HS^- \qquad E_0 = 0.90\ V \tag{15}$$

Only the additional assumption of a deprotonation, which is reasonable in a basic solution, provides redox potentials being able to reduce Co(II)Pc, calculated from Eqs. (14) and (15) by Nernst's equation

$$S^{-\bullet} + H^+ + e^- \rightleftharpoons HS^- \qquad E_{0,pH\,9} = 0.61\ V \tag{16}$$

$$HS_2^{2-\bullet} + H^+ + e^- \rightleftharpoons 2HS^- \qquad E_{0,pH\,9} = 0.369\ V \tag{17}$$

$$S_2^{3-\bullet} + 2H^+ + e^- \rightleftharpoons 2HS^- \qquad E_{0,pH\,9} = -0.162\ V \tag{18}$$

The overall potential for the oxidation of two HS^- to disulfide is $E_{0,pH\,9} = -0.233$ V at pH 9 [14]

$$S_2^{2-} + 2H^+ + 2e^- \rightleftharpoons 2HS^- \tag{19}$$

The considerations are summarized in the following reaction sequence for the sulfide oxidation catalyzed by Co(II)Pc

$$Co(II)Pc + HS^- \rightleftharpoons Co(II)Pc(HS^-) \tag{20}$$

$$Co(II)Pc(HS^-) + HS^- \rightleftharpoons Co(II)Pc(HS^-)_2 \tag{21}$$

$$Co(II)Pc(HS^-)_2 + 2OH^- \rightleftharpoons [Co(I)Pc(S_2^{3-\bullet})]^- + 2H_2O \tag{22}$$

$$[Co(I)Pc(S_2^{3-\bullet})]^- + O_2 \rightleftharpoons [(O_2)Co(I)Pc(S_2^{3-\bullet})]^- \tag{23}$$

$$[(O_2)Co(I)Pc(S_2^{3-\bullet})]^- + H_2O \rightarrow [(HO_2^{\bullet})Co(I)Pc(S_2^{2-})]^- + OH^- \tag{24}$$

$$[(HO_2^{\bullet})Co(I)Pc(S_2^-)]^- \rightarrow HO_2^- + Co(II)Pc(S_2^{2-}) \tag{25}$$

$$Co(II)Pc(S_2^{2-}) \rightleftharpoons Co(II)Pc + S_2^{2-} \tag{26}$$

The resulting reaction scheme is presented in Fig. 8. It considers spectroscopic results demonstrating the ready formation of Co(I)Pc in presence of HS^-, and, for the first time, reaction probabilities due to driving forces provided by published redox potentials for each of the individual steps of the reaction sequence.

The smallest driving force, i.e., $\Delta E_0 = 0.02$ V exists for the electron transfer from Co(I)Pc to O_2, which means that this reaction step might be the rate determining one. Indeed, electron transfer from Zn(II)Pc to adsorbed oxygen

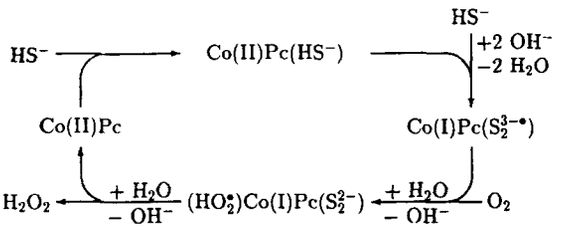

Figure 8. Reaction scheme of the catalyzed disulfide formation in the sulfide oxidation at pH 9.

was found to be the rate limiting step in the electrochemical reduction of oxygen on Zn(II)Pc thin films [33].

Since the coordinatively immobilized Co(II)Pc is as active as the dissolved one, although only one axial position is free for the coordination of the reaction partners, and since the adsorption of several partners is required during the oxidation sequence, the proposal of a Langmuir-Hinshelwood kinetics for this reaction seems to be adequate. So the main role of the phthalocyanine catalyst is to provide a transition complex with several educt molecules adsorbed simultaneously, not only at the Co center, but additionally at the extended π-electron system.

Presumably, the formation of zero valent sulfur is not a decisive intermediate, since it appeared in only one of the experiments using the highest catalyst concentration. In this case also the selectivity is changed drastically, resulting in the ratio sulfate/thiosulfate=0.17. The catalytic sulfide oxidation experiments, carried out under conditions where sulfur precipitation is avoided, do not alter the selectivity. This indicates that the catalyst affects only the bottle-neck of the oxidation reaction, i.e., the formation of disulfides [14].

It can be expected that the formation of the disulfides is catalyzed by Co(II)Pc, since this catalyst is well-known to produce disulfides from mercaptans [1, 28, 34]. As previously discussed in part I [14], the intermediate disulfide could not be detected, presumably, due to the high rates for the subsequent formation of polysulfides and oxidation to sulfate and thiosulfate.

5 Conclusions

Presumably, the mediation of the electron transfer in the Co(II)Pc-catalyzed sulfide oxidation proceeds via the redox change Co(II)Pc/Co(I)Pc and not via Co(III)Pc/Co(II)Pc as proposed previously [6], since a driving force exists for the former couple only.

The two-electron transfer to the dioxygen, i.e., the slowest step, requires a transition complex comprising several molecules, which could be provided with a higher probability by a catalyst, enabling the simultaneous adsorption of the reaction partners and being described more adequately by a simple Langmuir-Hinshelwood kinetics than by a Michaelis-Menten kinetics.

Thermodynamical data about the adsorption equilibria of the educts at the catalyst are obtained by this method and can be used in other systems.

The product ratio sulfate/thiosulfate=0.86, which is obtained for the uncatalyzed as well as the catalyzed process, indicates that the catalyst affects the rate determining step of the overall reaction only. The selectivity is obviously depending on the subsequent process.

Presumably, the intermediate disulfide is formed in the catalyzed rate determining step, since Co(II)Pc is known to promote the formation of disulfides.

Acknowledgment

Financial support by the Max Buchner-Forschungsstiftung (Project 1711) is gratefully acknowledged.

Received: April 21, 1997 [CET 908]

References

[1] Meyers, R.A., *Handbook of Petroleum Refining Processes*, McGraw-Hill, New York 1986.
[2] Kundo, N.N., Keier, N.P., *Kinet. Katal. 11* (1970) pp. 91–99.
[3] Hoffmann, M.R., Lim, B.C., *Environ. Sci. Technol. 13* (1979) pp. 1406–1414.
[4] Akhmadullina, A.G., Khrushchewa, I.K., Mazgarov, A.M., Abramova, N.M., *Khim. Tekhnol. Topl. Masel 8* (1985) pp. 42–43.
[5] Kochetkova, R.P., Shpilevskaya, L.I., Akhmadullina, A.G., Latyshev, V.P., Eppel, S.A., Mazgarov, A.M., *Zh. Prikl. Khim. 58* (1985) pp. 916–920.
[6] Kotronarou, A., Hoffmann, M.R., *Environ. Sci. Technol. 25* (1991) pp. 1153–1160.
[7] Hong, A.P., Boyce, S.D., Hoffmann, M.R., *Environ. Sci. Technol. 23* (1989) pp. 533–540.
[8] Simon, J., André, J.-J., *Molecular Semiconductors*, Springer, Berlin 1985.
[9] Leznoff, C.C., Lever, A.B.P., *Phthalocyanines, Properties and Applications*, VCH, New York 1989.
[10] Iliev, V., *J. Mol. Catal. 85* (1993) pp. 269–273.
[11] Wöhrle, D., Hündorf, U., Schulz-Ekloff, G., Ignatzek, E., *Z. Naturforsch. 41b* (1986) pp. 179–184.
[12] Buck, T., Bohlen, H., Wöhrle, D., Schulz-Ekloff, G., Andreev, A., *J. Mol. Catal. 80* (1993) pp. 253–267.
[13] Van Welzen, J., van Herk, A.M., German, A.L., *Makromol. Chem. 190* (1989) pp. 2477–2489.
[14] Fischer, H., Schulz-Ekloff, G., Wöhrle, D., Oxidation of Aqueous Sulfide Solutions by Dioxygen. Part I: Autoxidation Reaction., *Chem. Eng. Technol. 20* (1997) pp. 462 – 468.
[15] O'Brien, D.J., Birkner, F.B., *Environ. Sci. Technol. 11* (1977) pp. 1114–1120.
[16] La Mer, V.K., Kenyon, A.S., *J. Colloid Sci. 2* (1947) pp. 257–264. Cited after [15].
[17] Weber, J.H., Busch, D.H., *Inorg. Chem. 4* (1965) pp. 469–471.
[18] Buck, T., *Kovalent und koordinativ an Silicagel gebundene Metallporphyrine als Katalysatoren in der Thioloxidation. PhD Thesis*, Fachbereich 2, Universität Bremen 1992.
[19] Achar, B.N., Fohlen, G.N., Parkeer, J.A., Keshavayya, J., *Polyhedron 6* (1987) pp. 1463–1467.
[20] Buck, T., Preussner, E., Wöhrle, D., Schulz-Ekloff, G., *J. Mol. Catal. 53* (1989) pp. 17–19.

[21] van Herk, A.M., van Streun, K.H., van Welzen, J., German, A.L., *Brit. Polym. J. 21* (1989) pp. 125–132.
[22] Lasch, J., *Enzymkinetik — Eine Einführung für Biochemiker, Biologen, Chemiker und Pharmazeuten*, Springer, Berlin 1987.
[23] Bisswanger, H., *Theorie und Methoden der Enzymkinetik*. Verlag Chemie, Weinheim, 1979.
[24] Atkins, P.W., *Physical Chemistry*, Oxford University Press, Oxford, 3rd ed. 1986.
[25] Contour, J.P., Lenfant, P., Vijh, A.K., *J. Catal. 29* (1973) pp. 8–14.
[26] Fischer, H., Schulz-Ekloff, G., Buck, T., Wöhrle, D., Vassileva, M., Andreev, A., *Langmuir 8* (1992) pp. 2720–2723.
[27] Barzaghi, M., Beringhelli, T., Morazzoni, F., *J. Mol. Catal. 14* (1982) pp. 357–374.
[28] Fischer, H., Schulz-Ekloff, G., Buck, T., Wöhrle, D., *Erdöl, Erdgas, Kohle 110* (1994) pp. 128–135.
[29] Lever, A.B.P., Licoccia, S., Ramaswamy, B.S., Kandil, S.A., Stynes, D.V., *Inorg. Chim. Acta 51* (1981) pp. 169–176.
[30] Simonov, A.D., Keier, N.P., Kundo, N.N., Mamaeva, E.K., Glazneva, G.V., *Kinet. Katal. 14* (1973) pp. 988–992.
[31] Skorobogaty, A., Smith, T.D., *J. Mol. Catal. 16* (1982) pp. 131–147.
[32] Surdhar, P.S., Armstrong, D.A., *J. Phys. Chem. 90* (1986) pp. 5915–5917.
[33] Schlettwein, D., Jaeger, N.I., *J. Phys. Chem. 97* (1993) pp. 3333–3337.
[34] van Welzen, J., van Herk, A.M., Kramer, H., Thijssen, T.G.L., German, A.L., *J. Mol. Catal. 59* (1990) pp. 311–324.